Nanoscale

Cite this: *Nanoscale*, 2012, **4**, 394

www.rsc.org/nanoscale

COMMUNICATION

Polyvalent DNA–graphene nanosheets "click" conjugates†

Zihao Wang,‡ Zhilei Ge,‡ Xiaoxue Zheng, Nan Chen, Cheng Peng,* Chunhai Fan and Qing Huang*

Received 25th August 2011, Accepted 19th October 2011
DOI: 10.1039/c1nr11174d

Graphene is an increasingly important nanomaterial exhibiting great promise in the area of nanotechnology. In this study, the azide-functionalized graphene derivative was synthesized as the 'click' reagent for preparation of polyvalent DNA–graphene conjugates, which provide an effective and stable platform to construct new functional nano-architectures. Assembled with Au nanoparticles, the prepared Au–DNA–graphene nanocomplex exhibits excellent stability that could prevent the nanocomplex from being destroyed by surfactants. Assembled with DNA tetrahedron-structured probes (TSPs), the nanocomplex displays outstanding sensitive electrochemiluminescence properties, which might be used as a biosensor for DNA detection. Therefore, this DNA–graphene conjugates could be explored as the assembly unit for advanced DNA nano-architectures in the field of DNA nanotechnology.

Introduction

Graphene, an increasingly important two-dimensional (2D) nanomaterial with a single layer of carbon atoms,[1,2] has been actively explored for applications in numerous areas including field effect transistors, electromechanical resonators, micro-electro-mechanical systems (MEMS), ultrasensitive sensors,[3–9] and even in the field of biological and biomedical science due to its outstanding physical properties and good biocompatibility.[10–13] Graphene has also been intensively utilized as the 2D template to synthesize and prepare novel inorganic ultrathin 2D nanomaterials due to its unique one-atom-thick-2D chemical structure.[14–18] In previous efforts, we successfully constructed graphene-templated formation of high aspect ratio ultrathin single crystal lepidocrocite (gamma-FeOOH) nanosheets in aqueous solution phase.[14] Recently, Li *et al.* constructed DNA–graphene oxide nanocomplex *via* the noncovalent interaction of DNA strands with graphene oxide nanosheets showing high sensitivity and selectivity, for fabrication of ultrasensitive biosensors for DNA detection.[19] Until now, attention has been focused on achieving control over graphene with other exquisite nanoscale components to assemble precise and predictable architectures.

Laboratory of Physical Biology, Shanghai Institute of Applied Physics, Chinese Academy of Sciences, Shanghai, 201800, China. E-mail: huangqing@sinap.ac.cn; pengcheng@sinap.ac.cn

† Electronic supplementary information (ESI) available: Experimental procedures and additional materials. See DOI: 10.1039/c1nr11174d

‡ These authors have contributed equally to this work.

DNA nanotechnology has significant applications towards making functional nanomaterials because the unparalleled self-recognition properties of DNA offer the flexibility and convenience of the 'bottom-up' construction of exquisite nanostructures with high controllability and precision.[20–23] Therefore, high density covalent DNA–graphene conjugates may architecture high-ordered and multifunctional nanomaterials based on DNA technology.[19,24] To tightly build up DNA nanostructures on graphene, the primary unsolved problem is to form the solid DNA–graphene conjungation *via* strong covalent bonds. To the best of our knowledge, the present reports about biometric-mediated DNA assembly on graphene are all based on noncovalent interactions such as electrostatic force, Van der Waals forces, π–π stacks or hydrogen bonds,[19,24] which are insufficient to stabilize DNA–graphene nanocomplexes when in the presence of surfactants or in complicated surroundings such as organic solvents, cell sap or serum.[25] Therefore, intensive, nonaqueous, low selective synthetic methods such as acyl chlorination are not suitable for DNA-related chemical reactions.

The copper(I)-catalyzed azide-alkyne cycloaddition (CuAAC) 'click' reaction attracts great attention due to its high efficiency and specificity in the presence of many other functional groups.[26–28] Furthermore, the product of the reaction is the tolerant forms of triazole linkages, which is essentially inert to molecular oxygen, various solvents (including water), and under a vast array of conditions.[29–31] Therefore, these advantages make the 'click' reaction a versatile tool and the superior choice for attaching multifunctional molecules to functionalize the surfaces of many nanomaterials such as graphite,[32] carbon nanofibers,[33] carbon nanotubes,[34] gold,[35] silica[36] and magnetic nanoparticles (MNPs).[37] For example, Prosperi *et al.* reported carbohydrate and protein modified MNPs with highly conserved bioactivity through "click" reaction,[28] Mirkin and co-workers reported the synthesis of polyDNA–MNPs conjugates, which generated dense DNA-modified nanomaterials *via* 'click' reaction for cellular uptake without transfection reagents.[38] In this paper, we report an approach that utilizes graphene derivative functionalized with azides as the click reagent which can be rapidly coupled to alkyne-modified DNA strands to create stable polyvalent conjugates with exceptionally high DNA densities on graphene nanosheets. Importantly, this approach leads to DNA–graphene conjugates that exhibit excellent integration and stability of assembly with other multiple DNA nanostructures, which could be explored for advanced DNA nano-architectures on the 2D platform of graphene.

Experimental section

Materials

Graphite, 2-chloroethyl isocyanate, sodium azide and other chemical reagents were obtained from Sinopharm Chemical Reagent Co., the alkynyl functionalized DNA was synthesized and purified by TaKaRa Inc., and the sequences are shown in Table S1.† Dimethyl sulphoxide (DMSO) and N,N-Dimethylformamide (DMF) were dried under a molecular sieve before use and the solution of hydrogen peroxide was prepared daily. All other reagents were analytical grade and used as received. All aqueous solutions were prepared with Nanopure water (18 MΩ cm^{-1}) from a Millipore Milli-Q system.

Instruments

Atomic Force Microscopy (AFM) images were recorded using a Nanoscope IIIa apparatus (Digital Instruments, USA) equipped with a J Scanner. A droplet of each graphene derivative dispersion was cast onto a fresh mica surface, followed by drying at room temperature. The X-ray photoelectron spectroscopy (XPS) spectra of graphene derivatives were collected by using AXIS Ultra DLD (Kratos Co. Ltd., Britain). TEM samples were prepared by drop-casting AuNPs and DNA–graphene conjugate nanocomplex onto carbon coated copper grids. The images were recorded using a JEOL JEM 2011 microscope at an accelerating voltage of 120 kV. The UV–vis absorption data of the supernatant in AuNPs adsorption experiments were collected using a Hitachi U-3010 spectrophotometer (Hitachi Co. Ltd., Japan), and the fluorescence profiles of the supernatant in DNA adsorption experiments were measured with a Hitachi F-4500 fluorometer (Hitachi Co. Ltd., Japan).

Preparation of 2-chloroethyl isocyanate-treated graphene oxide (Cl–graphene)

Graphene oxide was synthesized following a modified Hummers' method,[39] and the 2-chlorethyl isocyanate-treated graphene oxide was synthesized as described in the literature.[40] In a typical procedure, 5 mL of graphene oxide in anhydrous N,N-dimethylformamide (DMF) (10 mg mL^{-1}) homogeneous suspension was loaded into a 10 mL round-bottom flask equipped with a magnetic stirring bar and then the organic 2-chloroethyl isocyanate (2 mmol) was added and the mixture was stirred under nitrogen. After 24 h, the slurry reaction mixture was poured into methylene chloride (50 mL) to coagulate the product. The product was then filtered, washed with additional methylene chloride (50 mL), and dried under vacuum.

Preparation of azide-functionalized graphene (Az–graphene)

To prepare azide-functionalized GO, 6 mmol sodium azide powders were added to 50 mg of Cl-graphene dissolved in 10ml of dimethyl sulfoxide (DMSO) after ultrasonication kept in an ice bath to prevent heating for 10 min, and then the mixture was stirred and refluxed for 48 h at 50 °C in a constant temperature oil bath, thus the azide group was introduced on the Cl-graphene sheets *via* nucleophile susbtitution reaction of alkyl halide. Followed by extraction with ethyl acetate to eliminate any residual DMSO, the black product was filtered and dried under vacuum.

Click reaction of alkyne-modified DNA and Az-graphene

The following solutions were made, respectively: (a) Az–graphene (1 mg L^{-1}); (b) alkynyl–functionalized DNA (1 μmol L^{-1}); (c) copper sulfate (2 μmol L^{-1}); (d) sodium ascorbate (10 μmol L^{-1}). The final solutions were made up in a constant amount ratio of 1(b) : 2(c) : 10 (d). Excess ascorbic acid was used to guarantee the complete reduction of copper sulfate. Then 50 μL of (a) was added to a 100 μL tube with 10 μL of (c) and 10 μL (d), and then 30 μL of (b) was added to the tube and stirred for 24 h at room temperature to obtain the click conjugates. The conjugates were centrifuged (10000 rpm, 10 min, room temperature) to be separated. After removing the supernatant, the conjugates was resuspended in 0.1 M PBS (pH = 7.4) to wash away the excess copper sulfate and sodium ascorbic acid.

The assembly between DNA–graphene conjugates and DNA–Au nanoparticles (AuNPs)

AuNPs of 15 nm were prepared as follows:[41] 3.5 mL of 1% trisodium citrate solution was added to a boiling and rapidly stirred solution of $HAuCl_4$, and the solution was kept boiling and stirred for 20 min. After being cooled to room temperature, the prepared AuNPs were stored at 4 °C. Then 6 μL of 100 μM thiolated DNA was added to the solution to a final concentration of 3 μM. After 16 h incubation at room temperature, the concentration of NaCl in the solution was brought to 0.1 M over a period of 24 h by stepwise addition of 1 M NaCl : 10 mM phosphate sodium buffer solution (pH = 7.4). Subsequently, 0.1 μM DNA–graphene conjugates were mixed with 0.3 μM DNA–AuNPs for hybridization. The assembly product of AuNPs and DNA–graphene would be easily separated by centrifugation because they were too heavy to suspend in solution. Therefore, the adsorption quantities of AuNPs assembly on graphene nanosheets could be measured by collecting the UV adsorption data of the suspensions after centrifugation. If AuNPs were present, UV adsorption at 550 nm would be detected because of the adsorption peak of the AuNPs.

Gel electrophoresis experiments

The 1% agarose gels were prepared for electrophoretic isolation of the assembled hybrid nanostructures formed between AuNPs and GO. After 20 μL of 1.5 μM GO–AuNPs conjugates were placed in the gels, they were run at 150 V in 0.5 × TBE (90 mM Tris : 89 mM boric acid : 2.0 mM EDTA, pH = 8.0) buffer for 60 min and examined under visible light.

The adsorption of DNA on DNA–graphene conjugate surfaces

10 μL of 10 μM fluorescence modified DNA (FAM-DNA) was added to the different volumes of Az–GO suspension after 'click' reaction with alkyne modified DNA. After the hybridization for 6 h, 1 × PBS (137 mM NaCl, 2.7 mM KCl, 100 mM Na_2HPO_4, 2 mM KH_2PO_4 pH 7.4) was added to the mixture till the volume of suspension reached 500 μL. Then the mixture was centrifuged (5000 rpm, 10 min, room temperature) to collect the hybridized GO and rinsed with 1 × PBS buffer. Subsequently, the GO part was collected carefully and added 100 μL of 1% SDS to release the non-hybridization-caused adsorbed FAM-DNA. The mixture was incubated for 12 h at room temperature with gentle shaking, and then centrifuged again to remove the upper suspension for fluorescence detection.

Formation of tetrahedron-structured DNA probes (TSPs)

The tetrahedrons were hierarchically assembled from three thiolated DNA fragments of 55 nucleotides (55-nt) and one probe-containing DNA fragment of 80-nt, which were mixed in stoichiometric equivalents in TM buffer (10 mM Tris-HCl, 50 mM $MgCl_2$), heated and then rapidly cooled to 4 °C. Of note, the tetrahedron assembly process was extremely fast (less than 2 min) with a high yield of over 85%.

DNA Immobilization and hybridization

The DNA tetrahedron-structured probes (TSPs) were assembled onto the Au surface by following the previous protocol.[21] In a typical experiment, the gold electrodes were polished using a microcloth, and rinsed with distilled water and ethanol. The sensing interface was fabricated as follows: 3 μL of 1 μM thiolated TSP oligonucleotide solution was added to each gold electrode overnight to establish the DNA nanostructure on gold surface. Then the DNA-modified electrode was incubated in 10 mM PBS (pH = 7.4, 0.3 M NaCl) containing the GO modified reporter DNA and 100 nM target solution at 25 °C for 2 h. Electrochemical measurements were taken just after all these treatments.

Electrochemical and Electrochemiluminescence (ECL) measurements

The ECL response was recorded by a CH151 Photon Detection Unit (Hamamatsu Photonics K.K., Japan) connected with a CHI 650 electrochemical workstation (CH Instruments Inc., Austin, TX). The conventional three-electrode system was composed of a modified gold electrode, an Ag/AgCl reference electrode (3 M NaCl) and a platinum counter electrode. Cyclic voltammetry (CV) was carried out at a scan rate of 100 mV s^{-1} between 0 and 0.8 V (*vs.* Ag/AgCl) and the ECL signal was recorded during the sweep. First, we checked the ECL in the presence of 200 μL luminol (l mM) but without H_2O_2, and then added 200 μL of 1μM H_2O_2 to 2 ml electrolyte. Compared with the non-complementary, mismatched, and no target samples, the 100 nM target revealed that they have different signal scale. In addition, all the experimental conditions, except the sequence design, are the same for the one base mismatched DNA, the non-complementary DNA and the target DNA.

Results and discussion

Synthesis of DNA–graphene conjugates

Graphene oxide (GO), the oxidized form of graphene, which contains hydroxyl, epoxyl and carboxyl functional groups as the positions for chemical modification, was prepared by a modified Hummers method and then used as the starting material. The synthesis route of DNA–graphene conjugates *via* CuAAC 'click' reaction in aqueous solution was designed as shown in Fig. 1. After the chemical treatment with 2-chloroethyl isocyanate, hydrophilic functional groups of GO were converted to hydrophobic functional groups, which enables Cl–graphene to be well dispersed in dimethyl sulfoxide (DMSO) and DMF (SI Fig. 1c†), but it cannot be dispersed in water or common polar protic solvents (SI Fig. 1b†). To examine the effect of charge from the azide functional groups, Az–graphene can be well dispersed in water (SI Fig. 1d†), which ensures 'click' reaction with alkynyl

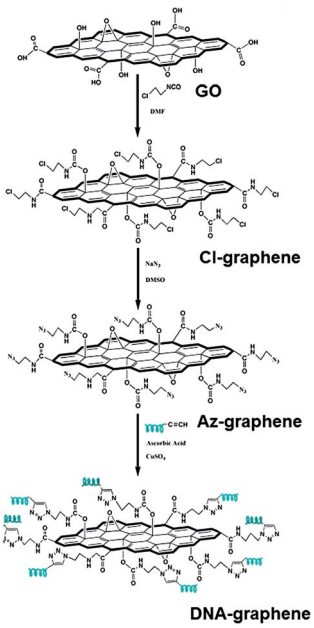

Fig. 1 Schematic representation of the synthesis route of DNA–graphene conjugates.

functionalized DNA in aqueous solution. However, considering the chemical cross-linking between the functional groups on GO nanosheets and the divalent or univalent copper ions,[42] the Az–graphene derivative formed irreversible flocky precipitates (SI Fig. 2†), which would no longer keep the 2D nanostructure of atomically thick graphene layers when copper ions were present in the aqueous solution. Therefore to avoid aggregation caused by copper ions, the other reactant alkynyl-functionalized DNA strands were mixed with Az–graphene before adding copper ions, because DNA could enhance the stability of Az–graphene as single layer suspending state in aqueous solution *via* facilitated non-covalent π–π stacking interactions.[43] The atomic force microscope (AFM) images of GO, Cl–graphene, Az–graphene and DNA–graphene (Fig. 2) demonstrated that the single layer feature of GO derivatives was definitely retained after the three steps of chemical reactions above. Furthermore, the thickness of DNA–graphene conjugates were 1.813 nm, while those of GO, Cl–graphene and Az–graphene were 1.110 nm, 1.215 nm, and 1.284 nm, respectively, indicating that the thickness increased due to chemical derivation.

The detailed structural and compositional analysis of DNA–graphene conjugates were further characterized and compared with Az–graphene, Cl–graphene and GO by X-ray photoelectron

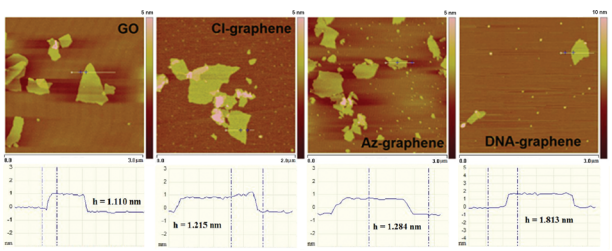

Fig. 2 Tapping-mode AFM image of as-prepared GO, Cl–graphene, Az–graphene and DNA–graphene conjugates.

spectroscopy (XPS). The carbon 1s spectrum of the GO starting material in SI Fig. 3† showed four components of the carbon bonds: sp2 hybridized carbon atoms of aromatic bonds (C═C, 284.9 eV), carbonyl bonds (C═O, 288.3 eV), hydroxyl bonds (C–O, 286.8 eV), and carboxylic bonds (O–C═O 289.2 eV). After isocyanate-treated reaction, the C 1s XPS spectrum of the chlorine replaced graphene derivative is shown in Fig. 3(a): the new peaks at 289.0 eV and 287.5 eV corresponded to the NH–C═O bonds and C–Cl bonds, respectively. Furthermore, the peak at 200.2 eV in the Cl 2p XPS spectrum (Fig. 3(b)) was associated with the bonds of Cl–C, which indicates the chlorine atoms were covalently bonded on the graphene nanosheets *via* isocyanate reaction. Fig. 3(c) and 3(d) are the C 1s and N 1s XPS spectra of Az–graphene. In detail, the peak at 286.6 eV in C 1s XPS spectrum represented the covalent form of C–N bonds on graphene nanosheets, which indicate that the chlorine atoms were replaced by azide groups. Moreover, the peaks at 398.6 eV and 402.8 eV in N 1s XPS spectrum (Fig. 3(d)) indicate that the azide groups were retained in the nucleophilic substitution reaction on graphene sheets. While after 'click' reaction, the obtained DNA–graphene conjugates showed distinguishable differences in XPS spectra: the peak appearing at 286.8 eV of DNA–graphene C 1s XPS spectrum in Fig. 3(e) was attributed to the bond of C–N, the peak appearing at 399.8 eV was attributed to N═N bond and the peak appearing at 401.5 eV was attributed to C–N bond in the N 1s XPS spectrum (Fig. 3(f)), which indicated the successful cyclization reaction between azide groups and alkynyl groups.

Nanocomplex of graphene nanosheets and AuNPs

Here, we construct the Au nanoparticles (AuNPs) and graphene nanocomplex (namely Au–DNA–graphene) *via* specific DNA hybridization interaction, the DNA–graphene nanosheets were synthesized above and the complementary DNA modified AuNPs were synthesized *via* thiol conjugation. Currently, focus is on the AuNPs and graphene nanocomplexes (namely Au–graphene) constructed by chemical or electrochemical deposition[44–46] and non-covalent interactions[47,48] for their wide potential applications in the field of Surface Enhanced Raman Spectroscopy (SERS)[49,50] and biosensors[51,52] *etc.* the AuNPs of the Au–graphene nanocomplexes made *via* chemical deposition are not uniform and the Au–graphene nanocomplexes made *via* noncovalent physical adsorption based on hydrophobic or π–π stacking interactions are not stable in the presence of surfactants. Thus, neither is suitable to construct more exquisite, more stable and more functional nanostructures. Here, the Au–DNA–graphene constructed by covalent DNA–graphene conjugates can retain the exquisite and stable nano-architectures in the presence of surfactants, based on the enhanced interactions between graphene nanosheets and AuNPs *via* strong chemical bond connection, which is much more stable and stronger than physical adsorption based on hydrophobic or π–π stacking interactions. The enormous differences between the transmission electron microscope (TEM) images of Au–DNA–graphene nanocomplex *via* a couple of pairing DNA strands and the TEM images of depairing DNA strands, both after washing with PBS buffer containing 1% Sodium dodecyl sulfate (SDS), are shown in Fig. 4(a) and Fig. 4(b), which clearly show that the high density AuNPs were well anchored on the graphene nanosheets *via* hybridization interaction of a couple of pairing DNA strands as the others were all removed by surfactant SDS. It is indicated that cooperating with DNA hybridization interactions, the covalent chemical bond connection of DNA–graphene is powerful enough to protect Au–DNA–graphene from the destruction due to the surfactant. We further investigated the electrophoretic separation experiments in an agarose gel and 1% SDS solution was used to test the stability of all nanomaterials. As shown in SI Fig. 4,† the marker of DNA modified AuNPs could easily penetrate the gel matrices so that an obvious reddish lane was observed by unaided eyes (lane 2), while the marker of DNA–graphene conjugates could not penetrate the gel matrices so that the

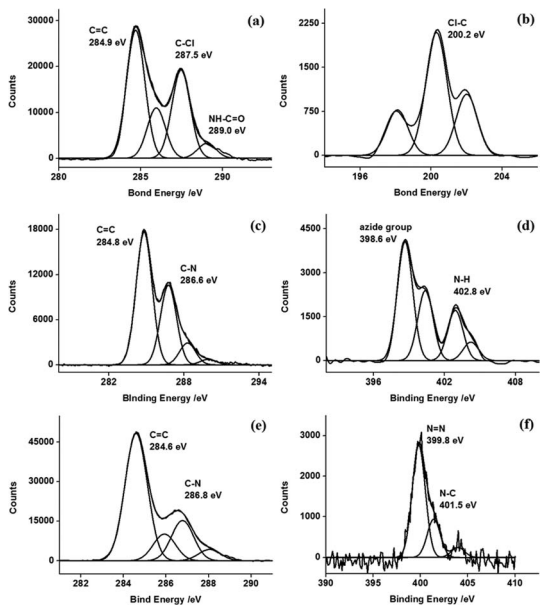

Fig. 3 XPS spectra of Cl–graphene (a: C, b: Cl), Az–graphene (c: C, d: N) and DNA–graphene (e: C, f: N).

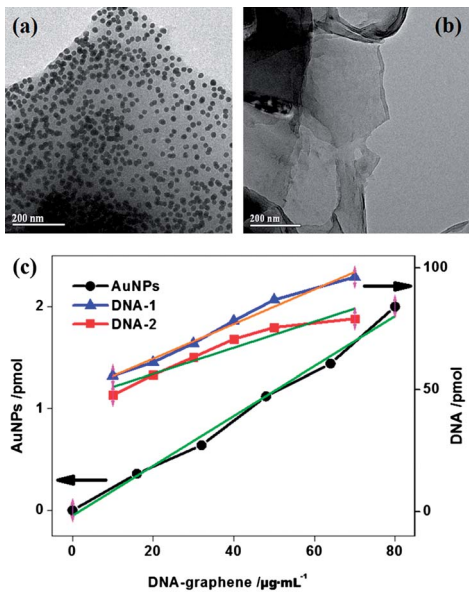

Fig. 4 TEM images of AuNPs–DNA–graphene nanocomplex (a) and AuNPs–graphene nanocomplex (b) after washing with PBS buffer containing 1% SDS solution; (c) is the adsorption isotherm of DNA and AuNPs on DNA–graphene nanosheets.

dark-brown DNA–graphene conjugates were stuck in the well (lane 1). Lanes 3 and 5 were loaded Au–DNA–graphene and Au–graphene mixers, respectively. After electrophoretic separation experiments, the good loading of Au–DNA–graphene remained red and dark-brown colors, which indicated that the AuNPs anchored on graphene were so well anchored that they could not be removed by the surfactant and driven into the gel matrix. However, the well in lane 5 that loading Au–graphene mixer represented a reddish band in the gel, which indicated the AuNPs were removed by surfactants and driven into the gel. Lane 4 was the sample of Au0–graphene after being washed by surfactant before electrophoretic separation experiments, because most of the AuNPs were removed by the surfactant, the remaining DNA–graphene were blocked in the well as the dark-brown color, which is the same as in lane 1. These results combined with the TEM images show that the DNA strands were firmly anchored on the graphene nanosheets *via* an efficient CuAAC 'click' reaction.

It is worth noting that a large quantity of conjugated DNA anchored on the graphene nanosheets *via* the 'click' reaction. Because graphene is a highly efficient fluorescence quencher, the quantity of conjugated DNA on DNA–graphene conjugates was evaluated by an indirect differential method *via* fluorescent measurements, and all the fluorescence intensities in the following experiments could be converted into corresponding DNA concentrations *via* the standard curve in SI Fig. 6.† In a typical experiment, a certain concentration of fluorescence modified complementary DNA (FAM-DNA) strand with a certain fluorescence intensity was added in the DNA–graphene conjugate suspension, and then the fluorescence intensity of the supernatant was measured after hybridization and centrifugation. The difference was equal to the sum of the quantity of specific hybridization and the quantity of nonspecific physical adsorption of π–π stacking or electrostatic interaction, which is shown as the blue curve in Fig. 4(c) (DNA-1). The precipitates were re-suspended and washed with buffer containing 1% of SDS surfactant to desorbed the nonspecific physical adsorbed FAM-DNA strands, and then the fluorescence intensity of the supernatant was recorded. After deduced by the curve DNA-1, the difference as shown in Fig. 4(c) red curve (DNA-2) was the pure quantity of DNA hybridization, which was equal to the conjugated DNA quantity on graphene nanosheets. Significantly in 1 mL system, the DNA strands conjugated on graphene nanosheets of 70 μg mL^{-1} could reach 79 pmol, which is a high enough density to assemble more complex nano-architectures with other materials such as AuNPs *via* DNA hybridization. The adsorption isotherm of DNA–graphene conjugates to AuNPs was also shown in Fig. 4(c) as the black curve, the quantity of AuNPs assembled on graphene nanosheets could reach about 2 pmol DNA–graphene at a concentration of 80 μg mL^{-1}.

Nanocomplex of graphene and 3D DNA nanostructure

Recently, DNA nanotechnology has gained great interest for developing functional 3D DNA architectures by building on the unparalleled high controllability and precision of the 'bottom-up' construction based on DNA self-recognition.[20,53] In particular, the pyramid-like DNA tetrahedron-structured probes (TSPs),[54,55] which are considered as highly rigid and versatile scaffolds in biosensors[21,23] for the detection of a broad range of biomolecules, because the well controlled spacing, high stability, and high density properties of TSPs assembled on the gold electrode offer a relatively thick solution-phase

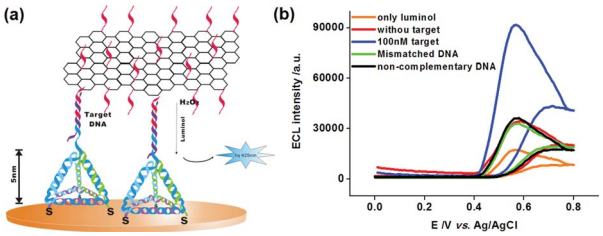

Fig. 5 Illustration of TSP–graphene nano-architecture (a) and ECL spectra of TSP–graphene (b).

layer still being amenable to electrochemical transduction and separating the probes from the complicated electrochemical interface environments to avoid interference from other biological macromolecules. In the following experiments, TSPs were integrated with DNA–graphene conjugates (TSP–graphene) *via* a conventional sandwich-DNA hybridization method on the gold electrode (Fig. 5 (a)), which exhibited an enhanced electrochemiluminescence (ECL) signal of luminol and H_2O_2, thus had potential applications in the field of biosensors. DNA–graphene conjugates retained the peroxidase-like catalytic activity of graphene oxide, which can catalyze the reduction of H_2O_2 leading to a characteristic blue color in the presence of H_2O_2 and a co-substrate 3,3′,5,5′-tetramethylbenzidine (TMB) (SI Fig. 5†). Furthermore, DNA–graphene retained excellent electron transfer property which completed the electron transfer from luminol oxidization to gold electrode through TSPs and DNA–graphene conjugates. As shown in Fig. 5(b), the ECL signal of TSP–graphene increased to more than 4 times that of luminol, while being more than twice the size of the ECL signals in the control experiments of non-complementary DNA and mismatched DNA. Therefore, this novel TSP–graphene nano-architecture constructed by DNA technology has such sensitive and precise properties that non-complementary DNA or even one base mismatched DNA strands can be detected.

Conclusion

We have demonstrated high density DNA functionalized graphene nanosheets for construction of complex nano-architectures. In this work, the copper-catalyzed azide-alkyne "click" reaction was used to conjugate DNA and graphene nanosheets. Importantly, the DNA–graphene conjugates showed effective and stable platform to construct new functional and complex nano-architectures *via* DNA hybridization. Importantly, the Au–DNA–graphene nanocomplex displayed excellent stability in the presence of surfactants, and the TSP–graphene nanocomplex exhibited outstanding sensitive ECL properties which might be a promising nanomaterial for a range of areas involving biosensors, nanorobots, and MEMS.

Acknowledgements

This work was financially supported by the National Natural Science Foundation (10905086, 10975179, 10905087, 90913014, 5102272, 31100716, 21105111 and 61008056), Ministry of Science and Technology (2006CB933000, 2007CB936000, 2007AA06A406), Shanghai Municipal Commission for Science and Technology (1052nm06100), Main Direction Program of Knowledge Innovation of CAS (Grant Nos: KJCX2-EW-N03), and the CAS innovation program.

References

1 A. K. Geim and K. S. Novoselov, *Nat. Mater.*, 2007, **6**, 183–191.
2 K. S. Novoselov, D. Jiang, F. Schedin, T. J. Booth, V. V. Khotkevich, S. V. Morozov and A. K. Geim, *Proc. Natl. Acad. Sci. U. S. A.*, 2005, **102**, 10451–10453.
3 K. S. Novoselov, Z. Jiang, Y. Zhang, S. V. Morozov, H. L. Stormer, U. Zeitler, J. C. Maan, G. S. Boebinger, P. Kim and A. K. Geim, *Science*, 2007, **315**, 1379.
4 K. S. Novoselov, A. K. Geim, S. V. Morozov, D. Jiang, Y. Zhang, S. V. Dubonos, I. V. Grigorieva and A. A. Firsov, *Science*, 2004, **306**, 666–669.
5 L. M. Lin, C. Dimitrakopoulos, K. A. Jenkins, D. B. Farmer, H. Y. Chiu, A. Grill and P. Avouris, *Science*, 2011, 327.
6 C. Lee, X. Wei, J. W. Kysar and J. Hone, *Science*, 2008, **321**, 385–388.
7 J. S. Bunch, V. D. A. Zande, S. S. Verbridge, L. W. Frank, D. M. Tanenbaum, J. M. Parpia, H. G. Craighead and P. L. McEuen, *Science*, 2007, **315**, 490–493.
8 M. D. Stoller, S. Park, Y. Zhu, J. An and R. S. Ruoff, *Nano Lett.*, 2008, **8**, 3498–3502.
9 J. B. Oostinga, H. B. Heersche, X. Liu, A. F. Morpurgo and L. M. K. Vandersypen, *Nat. Mater.*, 2008, **7**, 151–157.
10 W. Hu, C. Peng, M. Lv, X. Li, Y. Zhang, N. Chen, C. Fan and Q. Huang, *ACS Nano*, 2011, **5**, 3693–3700.
11 W. Hu, C. Peng, W. Luo, M. Lv, X. Li, D. Li, Q. Huang and C. Fan, *ACS Nano*, 2010, **4**, 4317–4323.
12 H. Wang, Q. Zhang, X. Chu, T. Chen, J. Ge and R. Yu, *Angew. Chem. Int. Ed.*, 2011.
13 C. Peng, W. Hu, Y. Zhou, C. Fan and Q. Huang, *Small*, 2010, **6**, 1686–1692.
14 C. Peng, B. Jiang, Q. Liu, Z. Guo, Z. Xu, Q. Huang, H. Xu, R. Tai and C. Fan, *Energy Environ. Sci.*, 2011, **4**, 2035–2040.
15 H. Wang, Y. Yang, Y. Liang, L. F. Cui, H. S. Casalongue, Y. Li, G. Hong, Y. Cui and H. Dai, *Angew. Chem.*, 2011, **123**, 7502–7506.
16 X. Huang, S. Li, Y. Huang, S. Wu, X. Zhou, S. Li, C. L. Gan, F. Boey, C. A. Mirkin and H. Zhang, *Nat. Commum.*, 2011.
17 H. Wang, J. T. Robinson, G. Diankov and H. Dai, *J. Am. Chem. Soc.*, 2010, **132**, 3270–3271.
18 X. Wang, S. M. Tabakman and H. Dai, *J. Am. Chem. Soc.*, 2008, **130**, 8152–8153.
19 L. Tang, Y. Wang, Y. Liu and J. Li, *ACS Nano*, 2011, **5**, 3817–3822.
20 P. W. Rothemund, *Nature*, 2006, **440**, 297–302.
21 H. Pei, N. Lu, Y. Wen, S. Song, Y. Liu, H. Yan and C. Fan, *Adv. Mater.*, 2010, **22**, 4754–4758.
22 Z. Ge, H. Pei, L. Wang, S. Song and C. Fan, *Sci. China Chem.*, 2011, **54**, 1273–1276.
23 P. Pei, W. Wan, J. Li, H. Hu, Y. Su, Q. Huang and C. Fan, *Chem. Commum.*, 2011, **47**, 6254–6256.
24 J. Liu, Y. Li, Y. Li, J. Li and Z. Deng, *J. Mater. Chem.*, 2010, **20**, 900–906.
25 M. Shim, N. W. S. Kam, R. J. Chen, Y. Li and H. Dai, *Nano Lett.*, 2008, **2**, 285–288.
26 H. C. Kolb, M. G. Finn and K. B. Sharpless, *Angew. Chem., Int. Ed.*, 2001, **40**, 2004–2021.
27 V. V. Rostovtsev, L. G. reen, V. V. Fokin and K. B. Sharpless, *Angew. Chem., Int. Ed.*, 2002, **41**, 2596–2599.
28 L. Polito, D. Monti, E. Caneva, E. Delnevo, G. Russo and D. Prosperi, *Chem. Commun.*, 2008, 621–623.
29 J. A. Opsteen, R. P. Brinkhuis, R. M. L. Teeuwen, D. W. P. M. Löwik and J. C. M. van Hest, *Chem. Commun.*, 2007, 3136–3138.
30 A. Dondoni, P. P. Giovannini and A. Massi, *Org. Lett.*, 2004, **6**, 2929–2932.
31 K. E. Beatty, J. C. Liu, F. Xie, D. C. Dieterich, E. M. Schuman, Q. Wang and D. A. Tirrell, *Angew. Chem., Int. Ed.*, 2006, **45**, 7364–7467.
32 A. Devadoss and C. E. D. Chidsey, *J. Am. Chem. Soc.*, 2007, **129**, 5370–5371.
33 W. H. Binder and R. Sachsenhofer, *Macromol. Rapid Commun.*, 2008, **29**, 952–981.
34 Y. Zhang, H. He, C. Gao and J. Wu, *Langmuir*, 2009, **29**, 5814–5824.
35 E. Boisselier, L. Salmon, J. Ruiz and D. Astruc, *Chem. Commun.*, 2008, 5788–5790.
36 L. Nebhani and C. Barner-Kowollik, *Adv. Mater.*, 2009, **21**, 3442–3468.
37 G. von Maltzahn, Y. Ren, J.-H. Park, D.-H. Min, V. R. Kotamraju, J. Jayakumar, V. Fogal, M. J. Sailor, E. Ruoslahti and S. N. Bhatia, *Bioconjugate Chem.*, 2008, **19**, 1570–1578.
38 J. I. Cutler, D. Zheng, X. Xu, D. A. Giljohann and C. A. Mirkin, *Nano Lett.*, 2010, **10**, 1477–1480.
39 W. S. Hummers and R. E. Offeman, *J. Am. Chem. Soc.*, 1958, **80**, 1339.
40 S. Stankovich, R. D. Piner, S. T. Nguyen and R. S. Ruoff, *Carbon*, 2006, **44**, 3342–3347.
41 L. M. Demers, C. A. Mirkin, R. C. Mucic, R. A. Reynolds, R. L. Letsinger, R. Elghanian and G. Viswanadham, *Anal. Chem.*, 2000, **72**, 5535–5541.
42 S. Park, K. S. Lee, G. Bozoklu, W. Cai, S. T. Nguyen and R. S. Ruoff, *ACS Nano*, 2008, **2**, 572–578.
43 A. J. Patil, J. L. Vickery, T. B. Scott and S. Mann, *Adv. Mater.*, 2009, **21**, 1–6.
44 K. J. Jeon and L. Lee, *Chem. Commun.*, 2011, **47**, 3610–3612.
45 X. Zhou, X. Huang, X. Qi, X. Wu, C. Xue, F. Y. C. Boey, Q. Yan, P. Chen and H. Zhang, *J. Phys. Chem. C*, 2009, **113**, 10842–10846.
46 C. Fu, Y. Kuang, Z. Huang, X. Wang, N. Du, J. Chen and H. Zhou, *Chem. Phys. Lett.*, 2010, **29**, 250–253.
47 X. Yang, M. Xu, W. Qiu, X. Chen, M. Deng, J. Zhang, H. Iwai, E. Watanabec and H. Chen, *J. Mater. Chem.*, 2011, **21**, 8096–8103.
48 J. Liang, Z. Chen, L. Guo and L. Li, *Chem. Commun.*, 2011, **47**, 5476–5478.
49 J. Huang, L. Zhang, B. Chen, N. Ji, F. Chen, Y. Zhang and Z. Zhang, *Nanoscale*, 2010, **2**, 2733–2738.
50 X. Fu, F. Bei, X. Wang, S. O'Brien and J. R. Lombardi, *Nanoscale*, 2010, **2**, 1461–1466.
51 J. H. Jung, D. S. Cheon, F. Liu, K. B. Lee and T. S. Seo, *Angew. Chem.*, 2010, **122**, 5844–5847.
52 W. Yang, K. Ratinac, S. Ringer, P. Thordarson, J. Gooding and F. Braet, *Angew. Chem., Int. Ed.*, 2010, **49**, 2114–2138.
53 D. Han, S. Pal, J. Nangreave, Z. Deng, Y. Liu and H. Yan, *Science*, 2011, **332**, 342–346.
54 R. P. Goodman, M. Heilemann, S. Doose, C. M. Erben, A. N. Kapanidis and A. J. Turberfield, *Nat. Nanotechnol.*, 2008, **3**, 93–96.
55 R. P. Goodman, I. A. T. Schaap, C. F. Tardin, C. M. Erben, R. M. Berry, C. F. Schmidt and A. J. Turberfield, *Science*, 2005, **310**, 1661–1665.